REFERENCES

Alcañiz-Monge, J., Lozano-Castelló, D., Cazorla-Amorós, D., and Linares-Solano, A. (2009). Fundamentals of methane adsorption in microporous carbons. Microporous and Mesoporous Materials, 124, 110-116.

Altenpohl, D., and Rogner, H-H. "Compressed natural gas (CNG): Potential applications for advanced transportation tanks and vehicle system." iiasa. June 1988. 15 May 2011.
<http://www.iiasa.ac.at/Admin/PUB/Documents/WP-88-047.pdf>

Arami-Niya, A., Duad, W.M.A.W., and Mjalli, F.S. (2011). Comparative study of the textural characteristics of oil palm shell activated carbon produced by chemical and physical activation for methane adsorption. Chemical Engineering Research and Design, 89, 657-664.

Azevedo, D.C.S., A,raújo, J.C.S., Bastos-Neto, M., Torres, A.E.B., Jaguaribe, E.F., and Cavalcante, C.L. (2007). Microporous activated carbon prepared from coconut shells using chemical activation with zinc chloride. Microporous and Mesoporous Materials, 100, 361-364.

Bagheri, N., and Abedi, J. (2011) Adsorption of methane on corn cobs based activated carbon. Engineering Research and Design, 89(10), 2038-2043.

Balathanigaimani, M.S., Kang, H-C., Shim, W-G., Kim, C., Lee, J-W., and Moon, H. (2006). Preparation of powdered activated carbon from rice husk and its methane adsorption properties. Korean Chemical Engineering, 23(4), 663-668.

Bao, Z., Yu, L., Ren, Q., Lu, X., and Deng, S. (2011). Adsorption of CO_2 and CH_4 on a magnesium-based metal organic framework. Journal of Colloid and Interface Science, 353, 549-556

Bastos-Neto, M., Canabrava, D.V., Torres, A.E.B., Rodriguez-Castellón, E., Jiménez-López, A., Azevedo, D.C.S., and Cavalcante, Jr., C.L. (2007). Effects of textural and surface characteristics of microporous activated carbons on the methane adsorption capacity at high pressures. Applied Surface Science, 253, 5721-5725.

Boyan, K., (2004). "Techno-economic analysis of natural gas application as an energy source for road transport in the EU." edis. Jan 2004 15 May 2011 <http://www.edis.sk/ekes/eur21013en.pdf>

Chen, Y., Zhu, Y., Wang, Z., Li. Y., Wang, L., Ding, L., Gao, X., Ma, Y., and Guo, Y. (2011). Application studies of activated carbon derived from rice husks produced by chemical-thermal process. Advances in Colloid and Interface Science, 163, 39-52.

Danna, A.B.M., Iyuke, S.E., Fakhrul-Razi, A., Chuah T.G., Atieh, M.A., and Al-Khatib, M.F. (2003). Synthesis and characterization of carbon nano-structures for methane storage. Environmental Informatics Archives, 1, 597-605.

Delavar, M., Ghoreyshi, A.A., Jahanshahi, M., and Irannejad, M. (2010). Experimental evaluation of methane adsorption on granular activated carbon (GAC) and determination of model isotherm. Engineering and Technology, 62, 47-50.

Duong, D.D. (1998). Adsorption analysis: Equilibria and kinetics. Queensland: Imperial college.

Dreisbach, F., Staudt, R., and Keller, J.U. (1999). High pressure adsorption data of methane, nitrogen, carbon dioxide and their binary and ternary mixtures on activated carbon. Adsorption, 5, 215-227.

El-Hendawy, A.A., Samra, S.E., and Girgis, B.S. (2001). Adsorption characteristics of activated carbons obtained from corncobs. A: Physicochemical and Engineering Aspects, 180, 209-221.

Esteves, I.A.A.C., Lopes, M.S.S., Nunes, P.M.C., and Mota, J.P.B. (2008). Adsorption of natural gas and biogas components on activated carbon. Separation and Purification Techology, 62, 281-295.

Farzad, S., Taghikhani, V., Ghotbi, C., Aminshahidi, B., and Nemati, L.E. (2007). Experimental and theoretical study of the effect of moisture on methane adsorption and desorption by activated carbon at 273.5 K. Journal of Natural Gas Chemistry, 16, 22-30.

Foo, K.Y., and Hameed, B.H. (2010). Insights into the modeling of adsorption isotherm system. Chemical Engineering Journal, 156, 1-10.

García, B.A.A., Alexandre, O.J.C., López, R., and Moreno- Piraján, J.C. (2010). A study of the pore size distribution for activated carbon monoliths and their relationship with the storage of methane and hydrogen. Colloids and Surfaces A: Physicochemical and Engineering Aspects, 357, 74-83.

Getzchmann, J., Senkovska, I., Wallacher, D., Tovar, M., Fairen-Jimenez, D., Düren, T., Baten, J.M.V., Krishna, R., and Kaskel, S. (2010) Methane storage mechanism in the metal-organic framework $Cu_3(btc)_2$: An in situ neutron diffraction study. Microporous and Mesoporous Materials, 136, 50-58.

Guo-Zhuo, G., Qiang, X., Yan-feng, Z., Shu-feng, Y., and Yun-fa, C. (2009). Regulation of pore size distribution in coal-based activated carbon. New Carbon Materials, 24(2), 141-146.

Kalderic, D., Bethanis, S., Paraskeva, P., and Diamadoporlos, E. (2008). Production of activated carbon from bagasse and rice husk by a single-stage chemical activation method at low retention times. Bioresource Technology, 99, 6809-6816.

Lozano-Castelló, D., Cazorla-Amorós D., and Linares-Solano, A. (2002). Powdered activated carbons and activated carbon fibers for methane storage. A comparative study. Energy & Fuels, 16, 1321-1328.

Morena-Castilla, C., Ferro-Garcia, M.A., Joly, J.P., Bautista-Toledo, I., Carrasco-Marin, F., and Rivera-Utrilla, J. (1995). Activated carbon surface modifications by nitric acid, hydrogen peroxide and ammonium peroxydisulfate treatments. Langmuir, 11, 4386-4392.

Moellmer, J., Moeller, A., Dreisbach, F., Glaeser, R., and Staudt, R. (2011) High pressure adsorption of hydrogen, nitrogen, carbon dioxide and methane on the metal-organic framework HKUST-1. Microporous and Mesoporous Materials, 138, 140-144.

Najibi, H., Chapoy, A., and Bahman, T. (2008). Methane/natural gas storage and delivered capacity for activated carbons in dry and wet conditions. Fuel, 87, 7-13.

Nour, U.M., Tayeb, A.M., Farag, A.H., and Awad, S. (2008). Enhanced discharge of ANG storage for vehicle use. Engineering and Technology, 9, 381-389

Paul, C.J., and Wu, S. (2004). Acid/Base-treated activated carbons: characterization of functional group and metal adsorption properties. Langmuir, 20, 2233-2242.

Prauchner, M.J., and Rodríguez-Reinoso, F. (2008). Preparation of granular activated carbons for adsorption of natural gas. Microporous and Mesoporous Materials, 109, 581-584.

Salehi, E., Taghikhani, V., Ghotbi, C., Lay, E.N., and Shojaei, A. (2007). Theoretical and experimental study on the adsorption and desorption of methane by granular activated carbon at 25°C. Journal of Natural Gas Chemistry, 16, 415–422.

Shao, X., Wang, W., and Zhang, X. (2007). Experimental measurements and computer simulation of methane adsorption on activated carbon fibers. Carbon, 45, 188-195.

Tancredi, N., Cordero, T., Rodríguez-Mirasol, J., and Rodríguez, J.J. (1996). Activated carbons from uruguayan eucalyptus wood. Fuel, 75(15), 1701-1706.

Wang, Y., Ercan, C., Khawajah, A., and Othman, R. (2012). Experimental and theoretical study of methane adsorption on granular activated carbons. AIChE Journal, 58(3), 782-788.

APPENDICES

Appendix A The Amount of Methane Adsorbed on all Adsorbents

Table A1 The amount of methane adsorbed on surface of metal organic framework from Basolite C300 at 303 K

Equilibirum pressure (psia)	Methane adsorption capacity (mmol/g)
0	0
24.38	1.75
45.01	2.87
60.01	3.70
90.01	4.72
121.88	5.67
157.51	6.75
196.88	7.68
240.01	8.47
286.88	9.11
333.76	9.62
384.38	10.13
436.88	10.56
495.01	10.90
575.63	11.27
675.01	11.55
766.88	11.74
868.13	11.96
997.51	12.15

Table A2 The amount of methane adsorbed on surface of metal organic framework from Basolite C300 at 308 K

Equilibirum pressure (psia)	Methane adsorption capacity (mmol/g)
0	0
22.5	1.41
45	2.57
63.75	3.24
91.88	4.19
121.88	5.08
157.5	6.15
196.88	6.94
238.13	7.68
283.13	8.40
330	8.93
382.5	9.51
431.25	9.85
493.13	10.20
570	10.49
663.75	10.78
763.13	10.98
862.5	11.17
965.63	11.31

Table A3 The amount of methane adsorbed on surface of metal organic framework
from Basolite C300 at 313 K

Equilibirum pressure (psia)	Methane adsorption capacity (mmol/g)
0	0
24.38	1.31
43.13	2.21
60	2.81
90	3.79
120	4.66
155.63	5.56
191.25	6.34
236.25	6.99
283.13	7.56
335.63	8.10
384.38	8.45
435	8.72
485.63	8.95
570	9.25
731.25	9.60
860.63	9.78
995.63	9.87

Table A4 The amount of methane adsorbed on surface of metal organic framework from Basolite Z1200 at 303 K

Equilibirum pressure (psia)	Methane adsorption capacity (mmol/g)
0	0
30	0.67
43.13	1.03
57.19	1.25
86.25	1.66
105	1.93
133.13	2.46
159.38	2.84
195.94	3.36
238.13	3.85
285	4.43
341.25	5.06
395.63	5.55
446.25	6.01
511.88	6.50
600	7.167
691.88	7.84
781	8.50
881.88	9.30
997.5	10.04

Table A5 The amount of methane adsorbed on surface of metal organic framework from Basolite Z1200 at 308 K

Equilibirum pressure (psia)	Methane adsorption capacity (mmol/g)
0	0
30	0.43
46.88	0.58
73.13	0.92
101.25	1.44
126.565	1.73
154.69	2.07
183.75	2.39
234.88	2.82
285	3.28
339.38	3.68
397.5	4.06
438.75	4.31
494.065	4.60
577.5	5.05
669	5.50
770.63	6.03
877.5	6.49
980.63	7.04

Table A6 The amount of methane adsorbed on surface of metal organic framework from Basolite Z1200 at 313 K

Equilibirum pressure (psia)	Methane adsorption capacity (mmol/g)
0	0
73.13	0.75
108.75	1.17
140.63	1.45
187.5	1.94
232.5	2.35
284	2.76
341.25	3.16
391.88	3.50
440.63	3.75
489.38	4.02
589.565	4.58
675.94	4.94
765.94	5.30
899.065	5.73
984.065	5.99

Table A7 The amount of methane adsorbed on surface of activated carbon from coconut shell powder at 303 K

Equilibirum pressure (psia)	Methane adsorption capacity (mmol/g)
0	0
15	0.86
28.13	1.35
54.38	2.01
84.38	2.55
110.63	2.92
135	3.16
163.13	3.40
183.75	3.54
208.13	3.71
247.5	3.95
301.88	4.22
345	4.39
399.38	4.58
451.88	4.76
500.63	4.89
586.88	5.04
678.75	5.14
768.75	5.21
873.75	5.27
982.5	5.28

Table A8 The amount of methane adsorbed on surface of activated carbon from coconut shell powder at 308 K

Equilibirum pressure (psia)	Methane adsorption capacity (mmol/g)
0	0
15	0.75
31.88	1.28
61.88	1.78
93.75	2.16
125.63	2.46
163.13	2.72
202.5	2.97
251.25	3.24
300	3.46
350.63	3.65
400.5	3.83
453.75	4.01
504.38	4.13
551.25	4.24
600	4.33
680.63	4.44
772.5	4.52
875.63	4.59
975	4.60

Table A9 The amount of methane adsorbed on surface of activated carbon from coconut shell powder at 313 K

Equilibirum pressure (psia)	Methane adsorption capacity (mmol/g)
0	0
15	0.71
31.88	1.11
60	1.63
93.75	2.01
133.13	2.35
165	2.56
202.5	2.76
247.5	2.97
300	3.18
350.63	3.36
393.75	3.49
448.8	3.60
498	3.71
575	3.84
673.13	3.96
772.5	4.04
871.88	4.09
990	4.10

Table A10 The amount of methane adsorbed on surface of activated carbon from calgon at 303 K

| Equilibirum pressure (psia)	Methane adsorption capacity (mmol/g)
0	0
20.63	1.13
37.5	1.62
61.88	2.14
80.63	2.40
108.75	2.78
136.88	3.10
166.88	3.38
198.75	3.66
243.75	4.00
292.5	4.27
337.5	4.49
393.75	4.71
446.25	4.89
498.75	5.02
571.88	5.19
669.38	5.35
763.13	5.46
864.38	5.54
988.13	5.61

Table A11 The amount of methane adsorbed on surface of activated carbon from calgon at 308 K

| Equilibirum pressure (psia)	Methane adsorption capacity (mmol/g)
0	0
38.25	1.41
69.38	2.07
106.88	2.57
166.88	3.13
226.88	3.51
301.88	3.89
397.5	4.25
511.25	4.55
624.38	4.76
725.63	4.86
815.63	4.90
909.38	4.92
997.5	4.92

Table A12 The amount of methane adsorbed on surface of activated carbon from calgon at 313 K

Equilibirum pressure (psia)	Methane adsorption capacity (mmol/g)
0	0
18.75	0.82
31.88	1.20
54.38	1.64
82.5	2.02
103.13	2.27
138.75	2.61
187.5	3.00
236.25	3.27
288.75	3.49
337.5	3.65
390	3.81
444.38	3.93
493.13	4.03
577.5	4.15
669.38	4.22
768.13	4.27
865	4.30
965.63	4.32

Table A13 The amount of methane adsorbed on surface of activated carbon from coconut shell particle at 303 K

Equilibirum pressure (psia)	Methane adsorption capacity (mmol/g)
0	0
17.815	1.07
30	1.58
58.13	2.24
86.25	2.78
103.5	3.10
148.13	3.74
191.25	4.19
242.815	4.60
286.88	4.89
341	5.17
423.75	5.55
496.88	5.82
590.63	6.09
682.5	6.30
780	6.43
888.75	6.52
995.75	6.53

Table A14 The amount of methane adsorbed on surface of activated carbon from coconut shell particle at 308 K

Equilibirum pressure (psia)	Methane adsorption capacity (mmol/g)
0	0
22.51	1.25
58.13	2.09
75.01	2.43
105.01	2.89
131.76	3.20
197.38	3.80
243.01	4.13
290.63	4.38
341.01	4.61
403.13	4.82
466.88	5.00
530.01	5.11
605.63	5.21
710.63	5.29
809.13	5.35
904.48	5.38
999.38	5.42

Table A15 The amount of methane adsorbed on surface of activated carbon from coconut shell particle at 313 K

Equilibirum pressure (psia)	Methane adsorption capacity (mmol/g)
0	0
20.63	0.80
56.25	1.60
78.75	2.01
103.13	2.37
138.75	2.77
185.63	3.12
234.38	3.45
296.25	3.76
359.065	4.01
410.13	4.16
471.565	4.28
565.88	4.36
669.88	4.43
765.5	4.47
864.38	4.50
992.815	4.53

Table A16 The amount of methane adsorbed on surface of activated carbon from eucalyptus at 303 K

Equilibirum pressure (psia)	Methane adsorption capacity (mmol/g)
0	0
24.38	1.231270224
33.75	1.518948133
58.13	2.057041033
84.38	2.500384804
108.75	2.879495133
148.13	3.33987313
193.13	3.773348836
245.63	4.136459309
288.75	4.447544818
343.13	4.738955803
393.75	4.992661534
444.38	5.203209185
491.25	5.361653016
573.75	5.623648698
665.63	5.849064984
763.13	6.055061345
866.25	6.241589443
965.63	6.350166618

Table A17 The amount of methane adsorbed on surface of activated carbon from eucalyptus at 308 K

Equilibirum pressure (psia)	Methane adsorption capacity (mmol/g)
0	0
24.38	1.068625283
33.75	1.373180001
58.13	1.748653994
88.13	2.179776017
112.5	2.572858864
150	2.982303436
196.88	3.285173435
243.75	3.618988328
294.38	3.911244378
343.13	4.138724711
391.88	4.368114413
481.88	4.705213234
562.5	4.961519464
665.63	5.228677624
761.25	5.407208634
862.5	5.55386248
969.88	5.629522201

Table A18 The amount of methane adsorbed on surface of activated carbon from eucalyptus at 313 K

Equilibirum pressure (psia)	Methane adsorption capacity (mmol/g)
0	0
26.25	0.839971344
35.63	1.004179219
56.25	1.433629408
84.38	1.892434824
105	2.195334656
146.25	2.577248764
200.63	2.997589526
249.38	3.309698195
289.5	3.575032526
341.25	3.840029774
390	4.068154827
442.5	4.275742068
494.13	4.422484681
575.63	4.651057937
669.38	4.850886306
774.2	4.988730117
865	5.07105764
961.88	5.126267361

- **Appendix B The Modeling and Experimental Data for Methane Adsorption Isotherm on all Adsorbents**
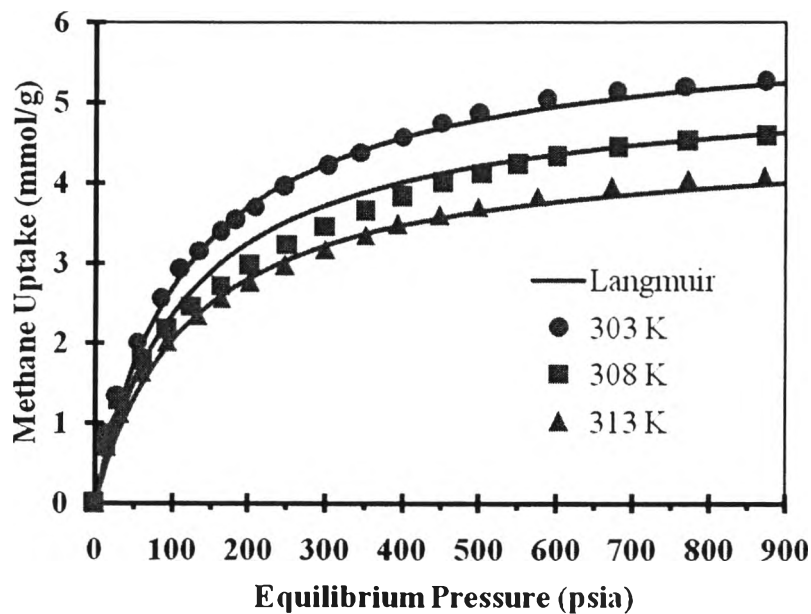
Figure B1 Methane adsorption on Coconut Shell Powder Activated Carbon. Symbols represent the experimental data while lines represent Langmuir isotherm model data.
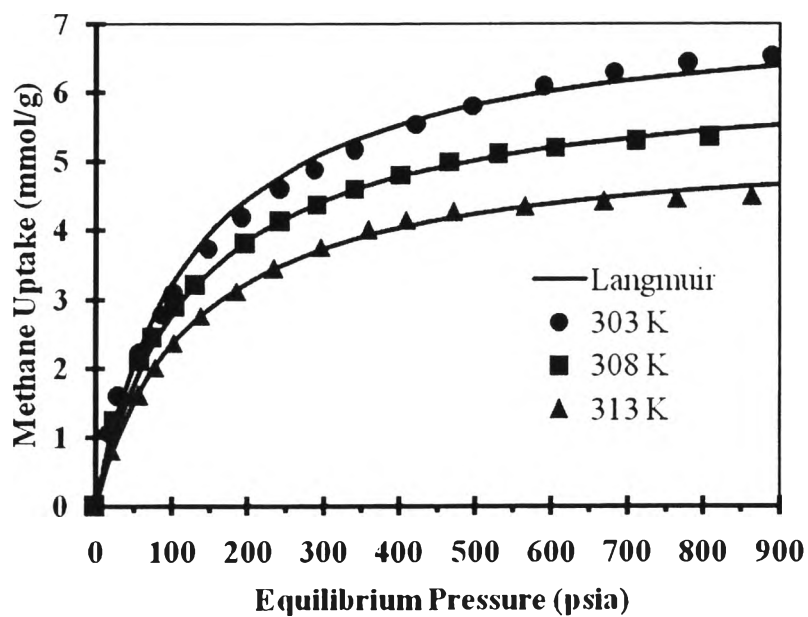
Figure B2 Methane adsorption on Coconut Shell Granular Activated Carbon. Symbols represent the experimental data while lines represent Langmuir isotherm model data.
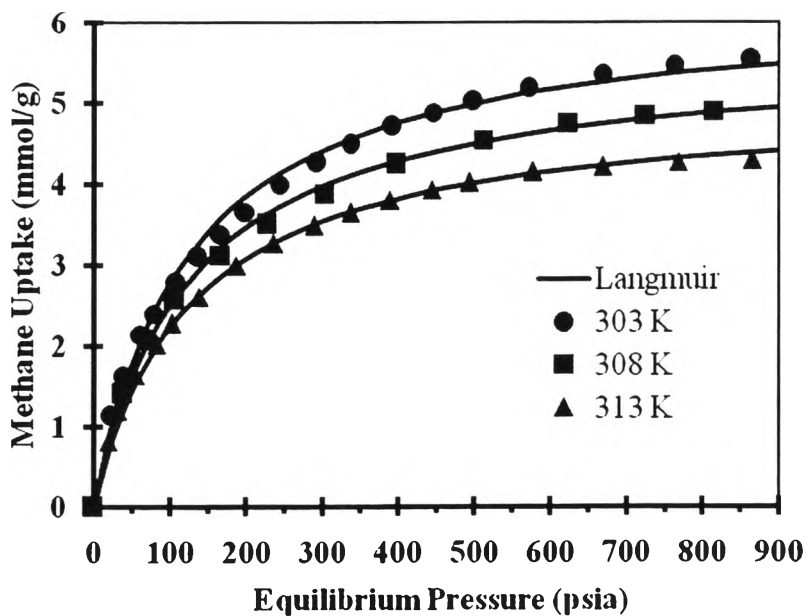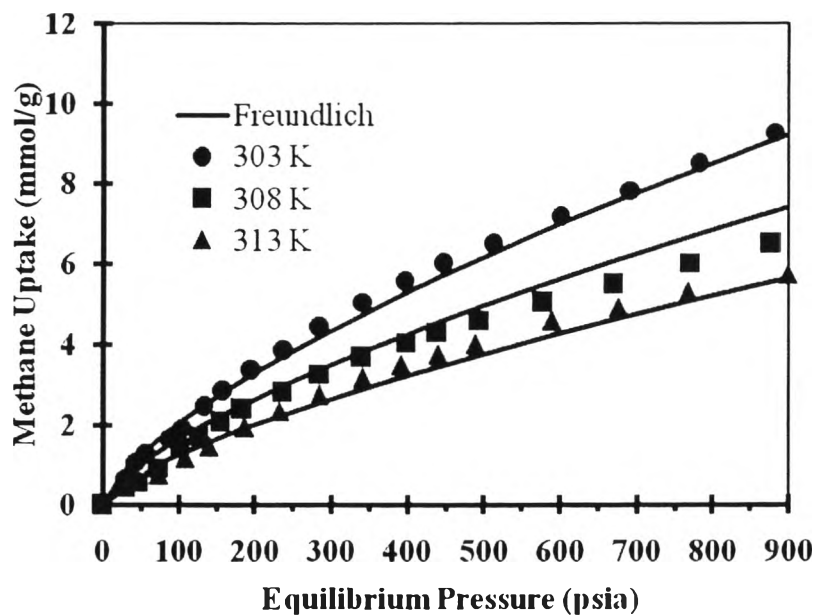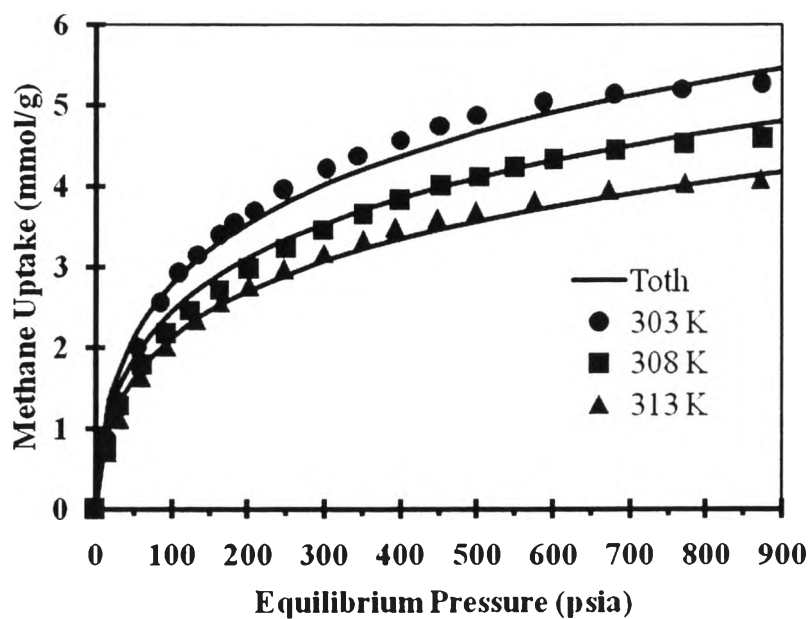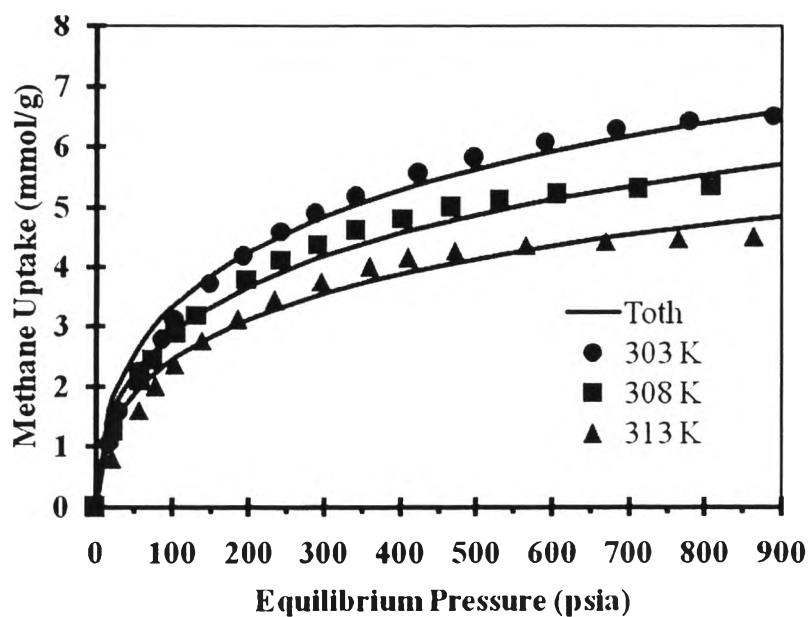

Figure B3 Methane adsorption on Calgon (20-40 meshes). Symbols represent the experimental data while lines represent Langmuir isotherm model data.
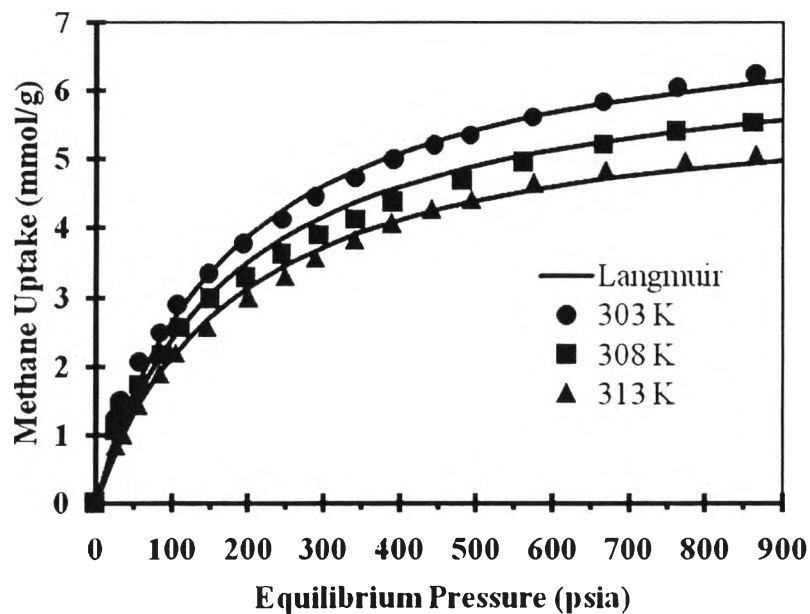
Figure B4 Methane adsorption on Eucalyptus Powder Activated Carbon. Symbols represent the experimental data while lines represent Langmuir isotherm model data.
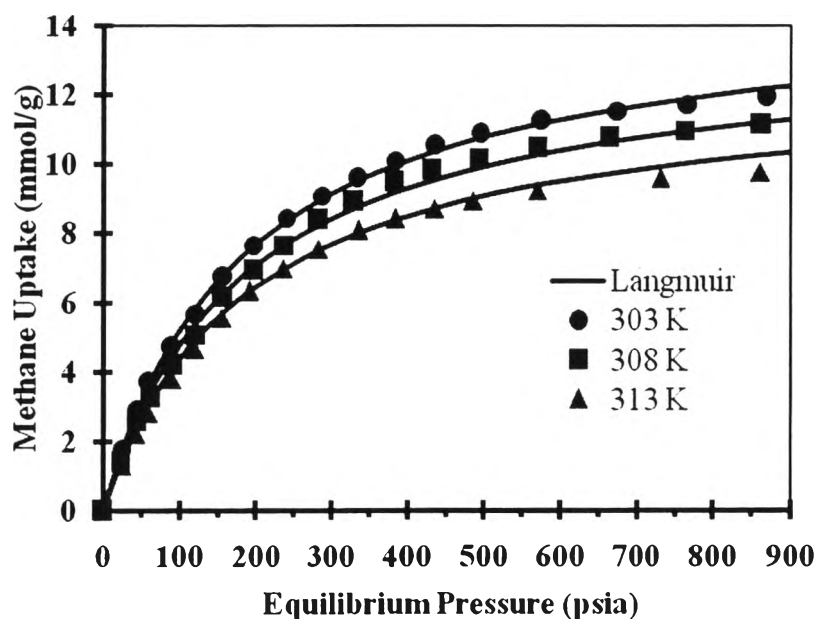
Figure B5 Methane adsorption on Basolite C300. Symbols represent the experimental data while lines represent Langmuir isotherm model data.
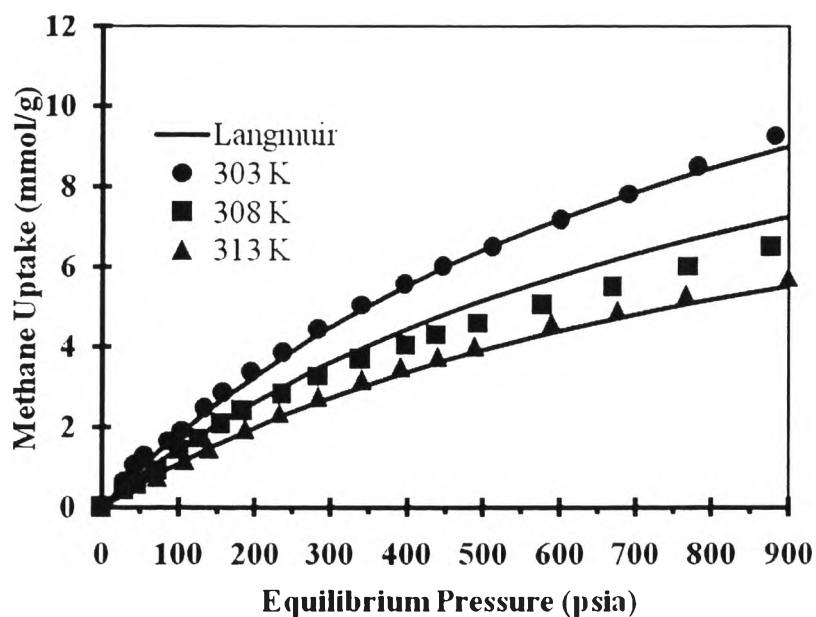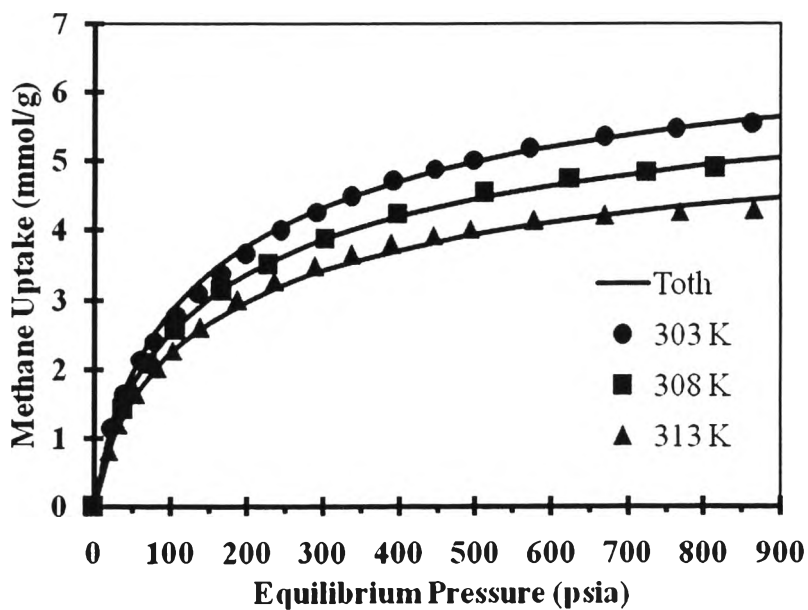
Figure B6   Methane adsorption on Basolite Z1200. Symbols represent the experimental data while lines represent Langmuir isotherm model data.
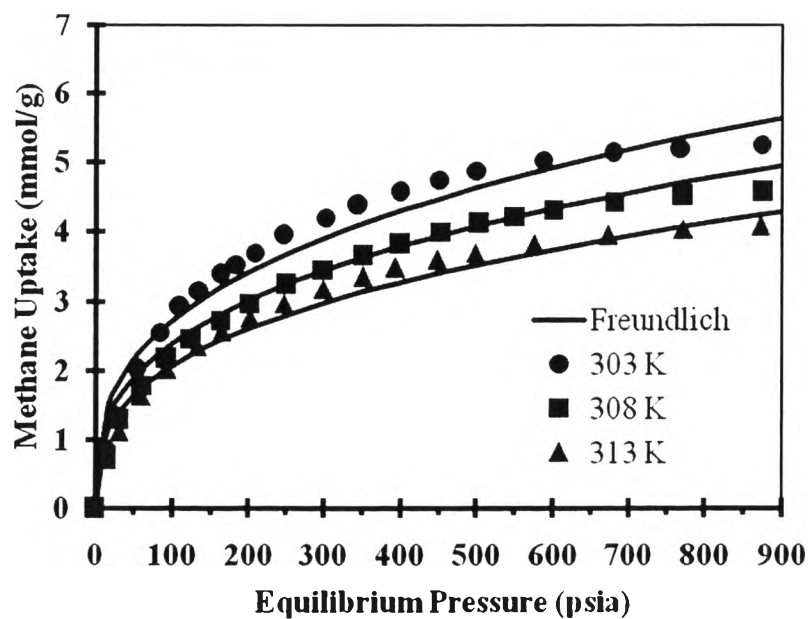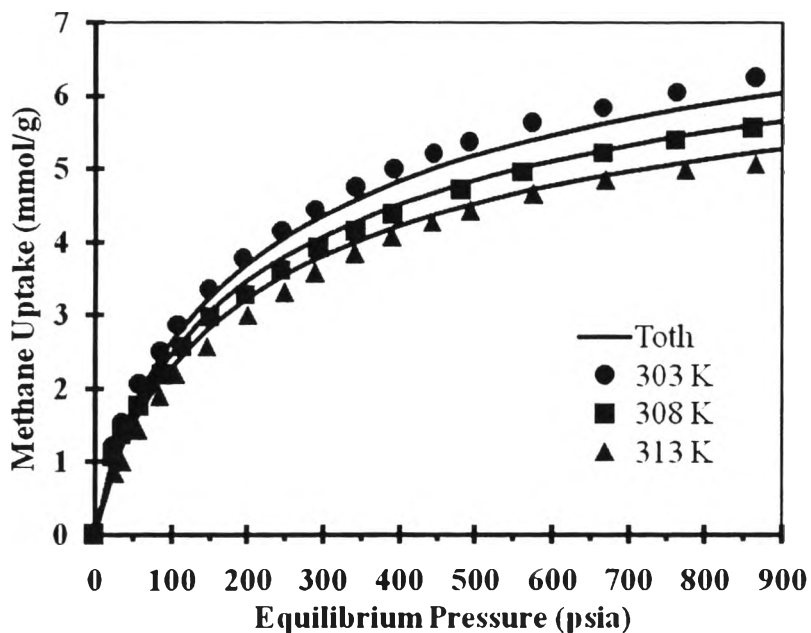

Figure B7   Methane adsorption on Coconut Shell Powder Activated Carbon. Symbols represent the experimental data while lines represent Freundlich isotherm model data.
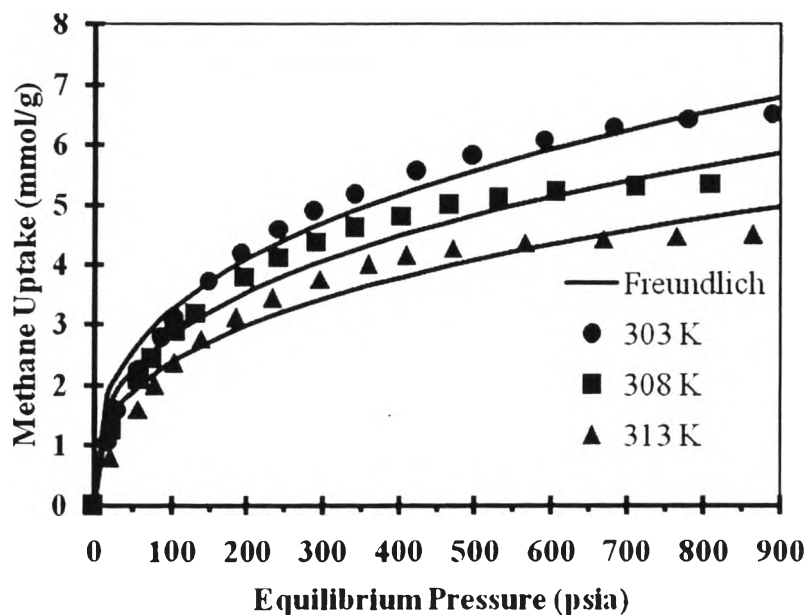
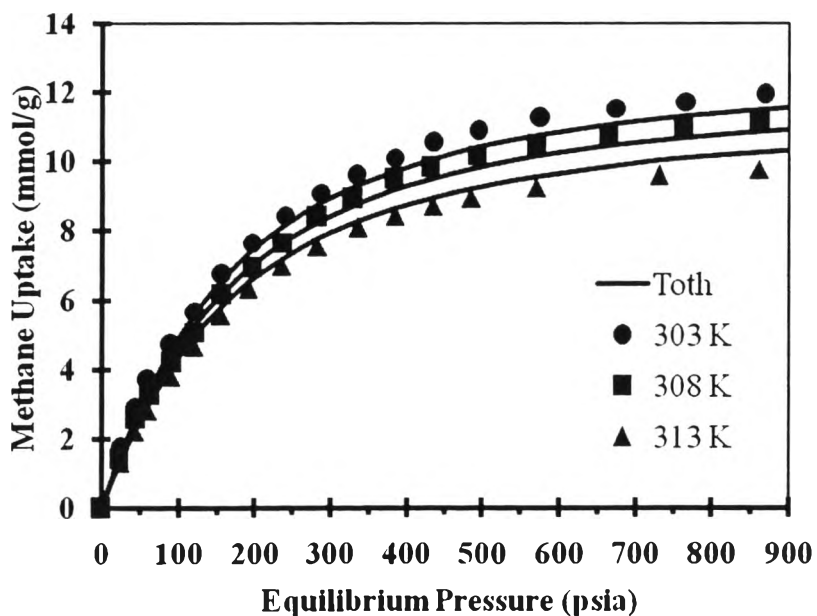**Figure B8** Methane adsorption on Coconut Shell Granular Activated Carbon. Symbols represent the experimental data while lines represent Freundlich isotherm model data.
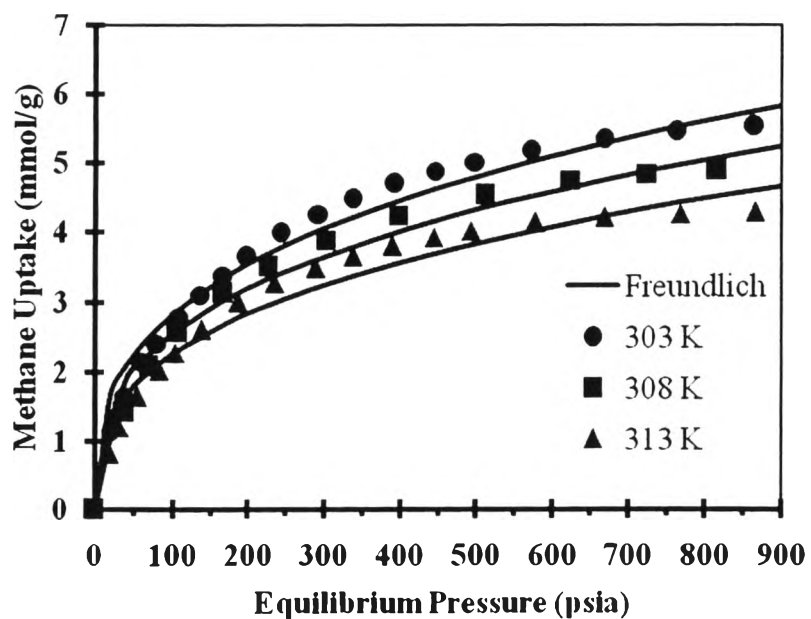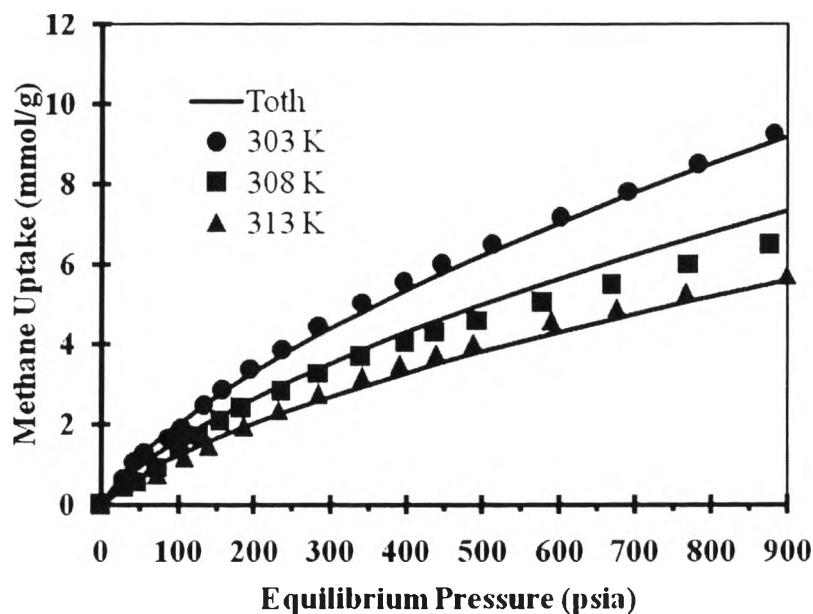

Figure B9 Methane adsorption on Calgon (20-40 meshes). Symbols represent the experimental data while lines represent Freundlich isotherm model data.
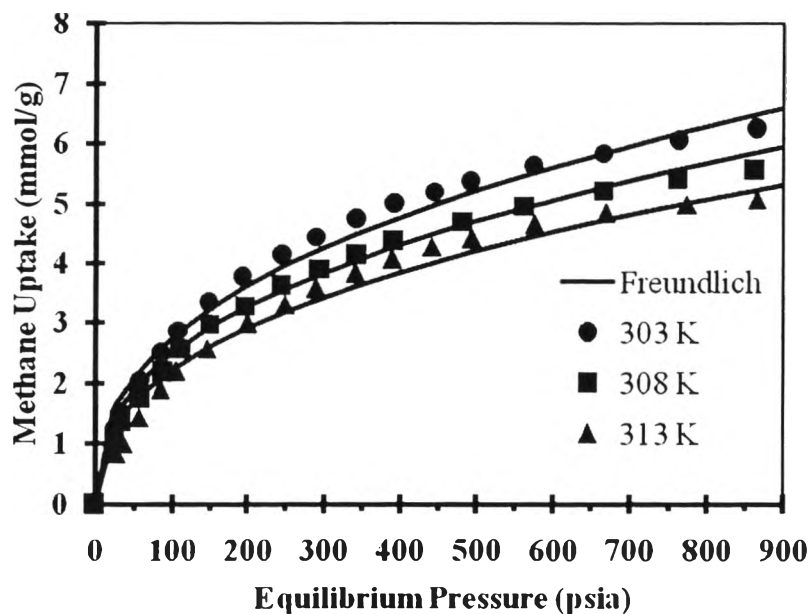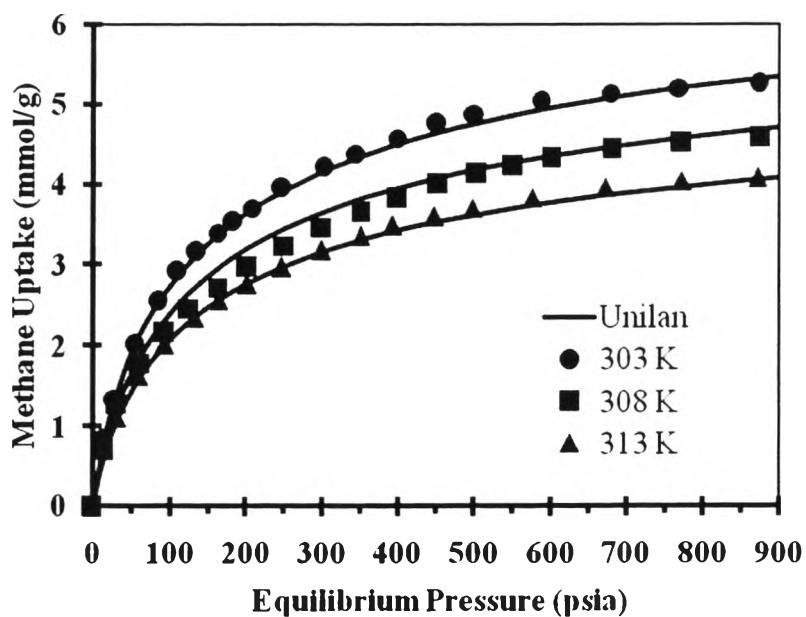
Figure B10 Methane adsorption on Eucalyptus Powder Activated Carbon. Symbols represent the experimental data while lines represent Freundlich isotherm model data.
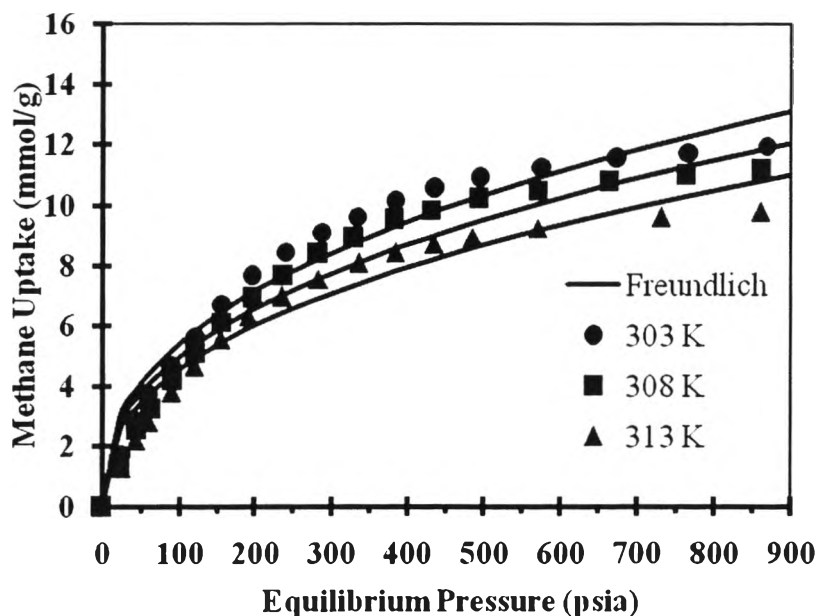
Figure B11 Methane adsorption on Basolite C300. Symbols represent the experimental data while lines represent Freundlich isotherm model data.
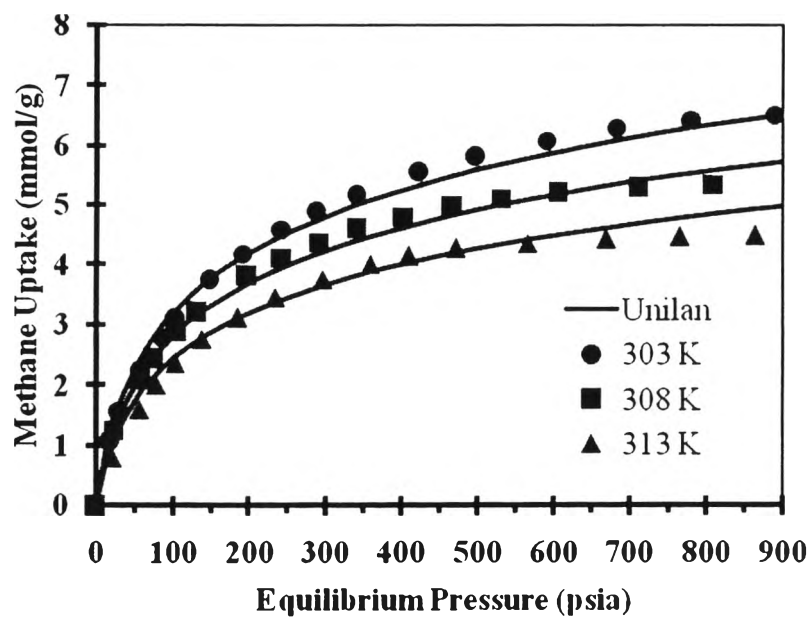
Figure B12   Methane adsorption on Basolite Z1200. Symbols represent the experimental data while lines represent Freundlich isotherm model data.

Figure B13   Methane adsorption on Coconut Shell Powder Activated Carbon. Symbols represent the experimental data while lines represent Toth isotherm model data.

Figure B14 Methane adsorption on Coconut Shell Granular Activated Carbon. Symbols represent the experimental data while lines represent Toth isotherm model data.

Figure B15 Methane adsorption on Calgon (20-40 meshes). Symbols represent the experimental data while lines represent Toth isotherm model data.

Figure B16 Methane adsorption on Eucalyptus Powder Activated Carbon. Symbols represent the experimental data while lines represent Toth isotherm model data.

Figure B17 Methane adsorption on Basolite C300. Symbols represent the experimental data while lines represent Toth isotherm model data.

Figure B18   Methane adsorption on Basolite Z1200. Symbols represent the experimental data while lines represent Toth isotherm model data.
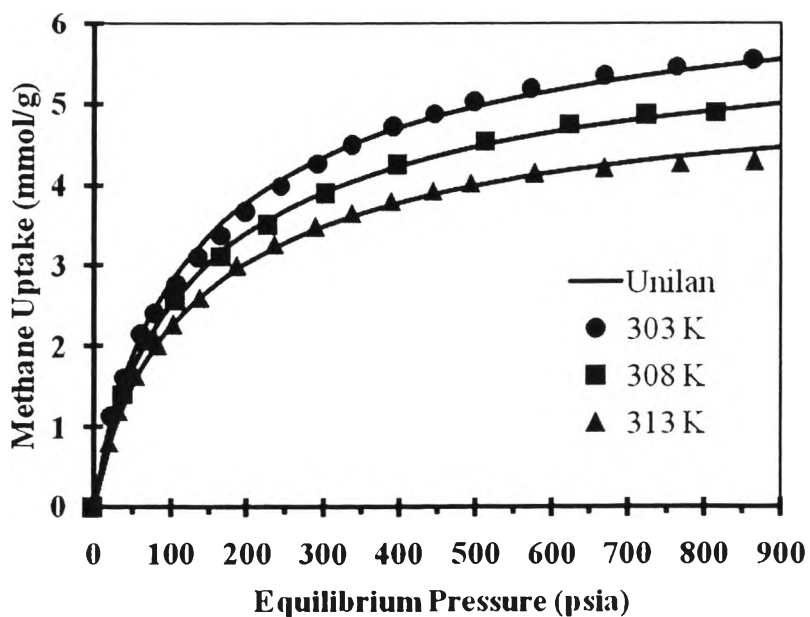

Figure B19   Methane adsorption on Coconut Shell Powder Activated Carbon. Symbols represent the experimental data while lines represent Unilan isotherm model data.
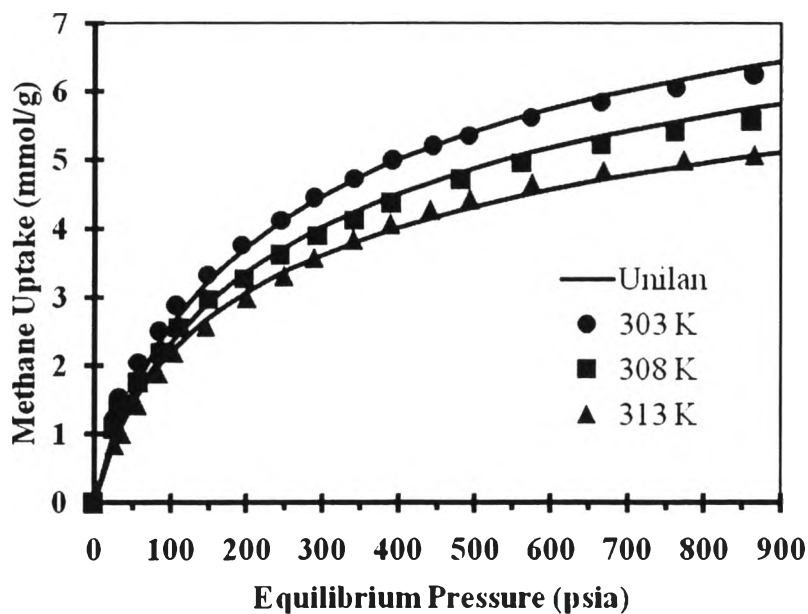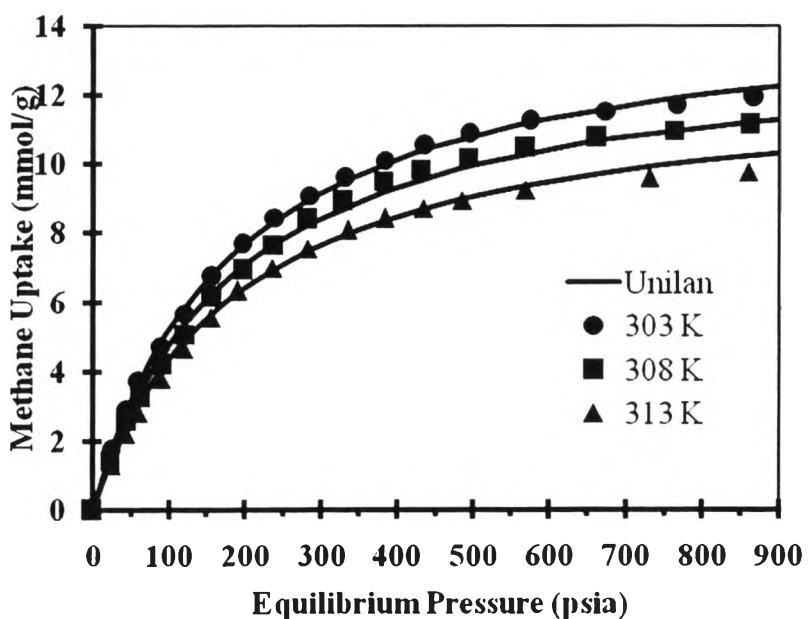
Figure B20   Methane adsorption on Coconut Shell Granular Activated Carbon. Symbols represent the experimental data while lines represent Unilan isotherm model data.
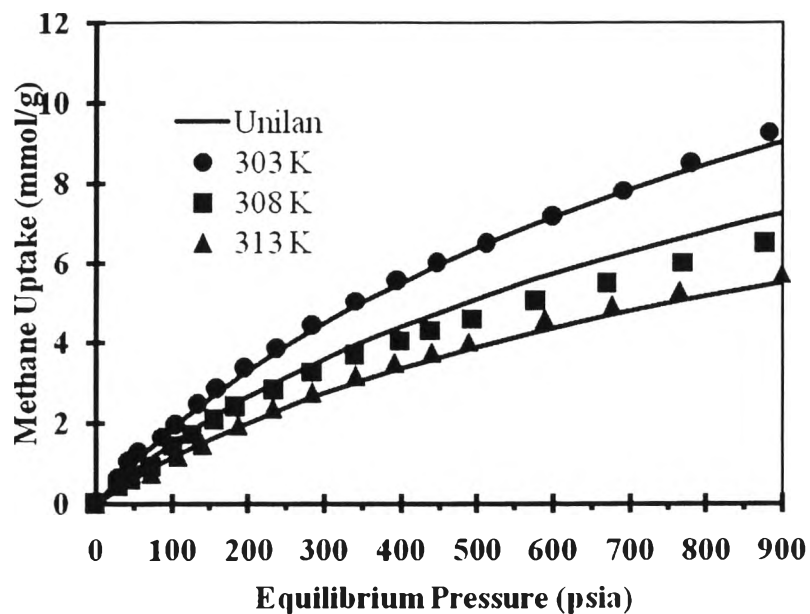

Figure B21   Methane adsorption on Calgon (20-40 meshes). Symbols represent the experimental data while lines represent Unilan isotherm model data.

Figure B22 Methane adsorption on Eucalyptus Powder Activated Carbon. Symbols represent the experimental data while lines represent Unilan isotherm model data.

Figure B23 Methane adsorption on Basolite C300. Symbols represent the experimental data while lines represent Unilan isotherm model data.

Figure B24 Methane adsorption on Basolite Z1200. Symbols represent the experimental data while lines represent Unilan isotherm model data.

CURRICULUM VITAE

Name: Ms. Narumol Kumpoomee

Date of Birth: March 7, 1988

Nationality: Thai

University Education:

2006–2010 Bachelor Degree of Petrochemical Engineering, Faculty of Engineering and Industrial technology, Silpakorn University, Thailand

Work Experience:

2009 Position: Engineer Internship Student

Company: PTT Aromatics and Refining Public Company Limited, Rayong, Thailand

Presentations:

1. Kumpoomee, N.; Kitiyanan, B.; Rangsunvigit, P.; and Kulprathipanja, S. (2012, April 24) Comparative Study of Methane Adsorption on Metal Organic Frameworks and Activated Carbons. Poster presented at The 3th Research Symposium on Petroleum, Petrochemicals, and Advanced Materials and the 18th PPC Symposium on Petroleum, Petrochemicals, and Polymers, Bangkok Thailand.